universität wien

MASTERARBEIT / MASTER'S THESIS

Titel der Masterarbeit / Title of the Master's Thesis

„Biomechanics of the shoulder and pectoral muscle during gliding flight in *Anhanguera piscator* (Archosauria, Pterosauria) from the Lower Cretaceous of Brazil"

verfasst von / submitted by

Florian Wegan BSc

angestrebter akademischer Grad / in partial fulfilment of the requirements for the degree of

Master of Science (MSc)

Wien, 2020 / Vienna 2020

Studienkennzahl lt. Studienblatt / degree programme code as it appears on the student record sheet:	A 066 815
Studienrichtung lt. Studienblatt / degree programme as it appears on the student record sheet:	Erdwissenschaften
Betreut von / Supervisor:	Univ.-Prof. Dr. Jürgen Kriwet

Content

1 List of Figures

2 Abstract

Pterosaurs were the first vertebrates to take active flight and they evolved into gigantic sizes during their occurrence in the Mesozoic era. Among them where the glider like ornithocheirid pterosaur family of Anhangueridae known from the Cretaceous of Brazil and Morocco. Their preferred style of flight is assumed to have been gliding or soaring long distances. In this thesis with the help of the fossil record and other publications, a research has been made on *Anhanguera piscator* to calculate the forces acting on the shoulder and pectoral muscle during gliding in this specimen and whether pterosaur experienced similar forces to modern birds. A life like 3D model of the wings of *Anhanguera piscator* was created and used to estimate the body mass and to calculate the lift generated by those wings. With the help of simple trigonometric functions, the forces the pectoral muscle had to generate, to keep the wing in an horizontal gliding position and the resulting stress in the articulation cartilage of the shoulder joint were determined. The pectoral muscle would have had to generate forces equal to nine or 12 times the body weight depending on the method used. At unsteady conditions, the values could spike up to 25 or 31 times the body weight, which is higher than in modern birds. The stresses on the gelnohumeral joint cartilage would range from 1,17 MPa to 3,78 MPa, which lies in range with modern animals.

3 Zusammenfassung

Flugsaurier waren die ersten aktiv fliegenden Wirbeltiere und entwickelten sich während ihres Auftretens im Mesozoikum zu gigantischen Größen. Unter ihnen waren die, ähnlich einem Gleitflugzeug, ornithocheirischen Flugsaurier aus der Familie der Anhangueridae, bekannt aus der Kreide Brasiliens und Marokkos. Es wird angenommen, dass der bevorzugte Flugstil das Gleiten war. In dieser Arbeit wurden, mithilfe von Fossilien und anderen Publikationen, die Kräfte untersucht, die während des Gleitens auf die Schulter und den Brustmuskel von *Anhanguer piscator* wirkten und ob diese Kräfte, mit denen moderner Vögel vergleichbar sind. Damit das Körpergewicht eingeschätzt werden konnte, wurde ein lebensechtes 3D Flügel-Model von *Anhanguera piscator* erstellt. Mithilfe dieses wurde auch der Auftrieb für jeden Flügel berechnet. Um zu erfahren welche Kräfte der Brustmuskel generieren musste um den Flügel in Gleitposition zu halten und welcher daraus resultierende Stress auf den Knorpel im Schultergelenk wirkte, wurden einfache trigonometrische Funktionen zu Hilfe genommen. Der Brustmuskel hätte das 9- bis 12-fache des Körpergewichts an Kraft generieren müssen, je nachdem welche Methode verwendet wurde. Unter turbulenten Bedingungen würden diese Werte bis auf das 25- bis 31-fache des Körpergewichts ansteigen und sind demnach höher als bei modernen Vögeln. Der Stress auf den Knorpel im Schultergelenk würde zwischen 1,17 MPa und 3,78 MPa liegen, welcher ähnlich dem moderner Tiere ist.

4 Introduction

Pterosaurs where the first vertebrates to take active flight. They began to evolve during the Triassic (245-205 Ma) and thrived during the Jurassic (205-145 Ma) and evolved into enormous sizes during the Cretaceous period (145-65 Ma) before going extinct alongside the dinosaurs at the end of that period, leaving the skies for others to rule (Witton, 2013). Their bizarre looking bodies, or what is left of them as bones, gave scientist a hard time to figure out their lifestyle and sparked many controversies in the past. Their body was highly altered and adapted for flight. They possessed small and short bodies, long necks, big heads, a fused coracoid and scapula, robust arm bones, an elongated forth finger to support a membrane, a pteroid bone in front of the wrist to support a small additional membrane (propatagium), a reduced and fused hip and slender leg bones (Benton, 2014). Pterosaurs underwent a distinct evolution in their body plan, as earlier forms were small and had proportionately long tails and small heads and later forms known as Pterodactyloidea, grew to much bigger sizes and had proportionately short tails and long heads. Transitional fossils show both basal and advanced traits (English & Middleton, 2015). The first fossils were discovered in the 18th century in the Jurassic limestones of Solnhofen, Germany. Cuvier (1801) was the first to point out their reptilian traits and later in the 19th century they got their name “winged lizards” or Pterosauria. Since then many different groups all over the world were discovered with different styles of feeding and head morphologies (Benton, 2014). Only during the 1930s to 1960s the interest in pterosaurs decreased and not a lot of contributions have been made, to further understand those bizarre creatures. Since the 1970s the interest in pterosaurs reappeared thanks to the magnificent work of Peter Wellnhofer. The progress in this field of research hasn´t stopped and thanks to technical advances like computer-tomography or scanning electron microscopes and advanced computational methods even accelerated progress and insight (Witton, 2013).

Today the majority of pterosaur paleontologists agree that pterosaurs were built for flight and were able to fly as efficient as modern birds. There is even evidence that the biggest pterosaurs with 10 m wingspan and body weights of up to 250 kg were able to fly. To get airborne birds propel themselves into the air by generating an initial power with the help of their hind limbs and pterosaur most likely used a quadrupedal launch mechanism just as some bats do. Pterosaurs did not rely on feathers but on a membrane to provided lift, which means that they needed to adopt different principles

to stay airborne (Benton, 2014). Three basic parameters have to be known to study flight, which are the wingspan, wing area and the body mass. The first two aspects could be referred from the fossil record but the body mass is and always has been a highly controversial and speculative topic in this field of research. There are many different approaches to this problem and body masses can differ by the twofold (Witton, 2013). In this study *Anhanguera piscator*, a member of the ornithocheirid family was used to study the biomechanics of the shoulder and the pectoral muscle during flight or to be more precise during gliding flight. An anhanguerid species was chosen for this project, as its expected style of flight seems to have been gliding or soaring. From this, the question arises, if pterosaurs experienced the same forces during flight in the shoulder and the pectoral muscle as birds do today.

The Null-Hypothesis will be that the pectoral muscle of pterosaurs experience the same relative, to their body weight, forces as seen in modern birds during gliding.

5 Material & Methods

5.1 Pterosaur cast:

The specimen used for this project is a cast of *Anhanguera blittersdorffi* (Campos & Kellner, 1985) which was obtained by the University of Vienna from the University of Frankfurt am Main more than 20 years ago in exchange for other casts (for example a cave bear). The specimen shown at the Geological Department of the University of Vienna in Spittelau (UZA2) is a detailed copy of the original reconstruction in Frankfurt. The original cast was a donation made by the Lions club Frankfurt am Main to the Museum in Frankfurt am Main and is representing a pterodactyloid pterosaur from the Aptium, Later Cretaceous from the Sanatana-Formation in Brazil. More precisely from the Chapada do Araripe, Romualdo Member also known as Araripe Plateau from Ceará, Brazil (Fossilworks, n.d). The Lions Club Frankfurt am Main is a non-political organization that according to their motto “we serve“, stands for an active contribution to the evolution and advancement of society (Lions Club Frankfurt am Main, 2013).

5.2 Casts of humerus and scapulacoracoid

The humerus (upper arm) and the scapulacoracoid (fusion between the shoulder blade and the coracoid) were wrapped tightly with a two component silicone rubber that vulcanizes at room temperature, called ELASTOSIL® M 1470 from Wacker Chemie to capture all significant characteristics. The pink kneadable rubber could be applied to the surface of the bones without much preparation. ELASTOSIL® M 1470 has a high Shore A hardness of approx. 45, good heat resistance and low shrinkage and was therefore perfect to be used as a molding material. The bones were covered with a small layer of a mixture of Vaseline and benzine, so that the rubber after curing did not stick to the bones. With the addition of a Catalyst (for example in this case Paste T 40) the curing time was somewhere between one to five hours depending on how much paste was used. For this project, the rubber cured over night to make sure that it fully vulcanized. Half a kilogram of rubber were used for this process. After the curing process was completed, the rubber coatings were cut off the cast into two pieces, one was the humerus and the second part was the scapulacoracoid.

The next step was to poor the actual casts that can be worked with. For this purpose, the marble filler 1000 from AKEMI in jura light was used because, it is a liquid, creamy two-component polyester resin, so it was possible to cover even the smallest details of the mold. After hardening, it provides a hard model, which can be sanded or altered in many other ways to attain a model as similar as possible to any fossil references. For the humerus rubber coating the distal opening was sealed with silicon. The mold was than brushed with a thin layer of marble filler 1000 Universal from AKEMI to avoid air bubbles on the surface. Quickly the mold was fixed with cable ties so that the Marble Filler can´t leak out and the mold was held together at the cutting edges on the dorsal side of the humerus. Caution was advised to not put too much pressure on the mold with the cable ties so that the original shape was obtained. The mold was held in a vertical position and the marble filler 1000 Universal was poured into the proximal, in vertical position the top, opening. About a whole one kg can was used to fill the mold. To allow fast hardening, a hardening Paste from AKEMI was added to the marble filler. After 20 - 40 Minutes the liquid was hardened and ready to be further processed. For the scapulacoracoid, similar steps were taken to get the cast. The opening where the sacpulacoracoid meets the sternum was filled with marble filler and hardened to seal the opening. To make this process easier the sternum was molded as part of the scapulacoracoid in the previous step to allow an easy solution to close that hole in the rubber mold. So even a part of the sternum was molded and casted but will not be over other significance in this study. With cable binder the rubber shell was held together to prevent leaking at the lines of cutting. All other holes except of two were closed with silicon, so that only one at the most dorsal and most proximal part, where the scapula would articulate with the notarium, and the most distal part of the scapulacoracoid, where the glenoid fossa is built by the coracoid and scapula, were left open, to later fill in the fluid marble filler. It was not necessary to coat the inner side of the rubber mold, because the model needs remodeling anyway and therefore little air bubbles on the surface could be tolerated. The marble filler was poured in two stages. First, the coracoid part, through the most distal hole at the glenoid fossa and after a few minutes of hardening this hole was closed with modelling clay so that in a second step the scapula part of the model was filled with marble filler through the most proximal dorsal hole. After 20 - 40 minutes, the model was finished and could be taken out of the rubber mold and further processed. Even though it was necessary to make a new model it was decided to start with the cast of the original model and work from there with the help of modelling clay, to work out the best possible form.

5.2.1 Modeling of humerus

The humerus cast was 24 cm in length and had a wrapped deltopectoral crest. The humeral head was shaped like a kidney and the articular surface was convex. The humeral shaft was twisted ventrally to the humeral head. The deltopectoral crest takes up 34% of the humeral shaft length. These characteristics are typical for ornithocheiroid pterosaurs (Elgin & Frey, 2011).

The model was sanded and freed from any little irregularities. The caput humeri was smoothened and changed to match the description and the pictures of Kellner & Tomida (2000).

5.2.2 Modeling of scapulacoracoid

The scapulacoracoid had a scapula length of 10 cm and a coracoid length of 12 cm. This model was used as a basic framework and with the help of modelling clay, the model was changed according to the pictures and description in Bennett (2003). The first step was to model the overall shape of the scapulacoracoid to match the pictures and the different angles. To start with, the whole model was adjusted to the coracoid, which was used as a benchmark. The ventral medial articular surface where the coracoid articulates with the sternum was not modeled because it is not necessary for this study to do so. The same applies to the ventral most proximal surface where the scapula articulates with the Notarium. The scapula was rotated caudodorsally so that it clearly offsets with the coracoid when viewed from lateral. The posterior margin of the scapula with the prominent tubercle and the posterior articular surface of the glenoid surface was molded next, followed by the missing part of the glenoid fossa and superior and anterior to it a prominent rounded process. Finally yet importantly, the biceps tubercle was attached. After the general form of the model matched those of the drawings in Bennetts´ paper from 2003 a new mold was formed.

The model was placed on a, previously rolled out about 3 cm thick plate of modelling clay and covered with a mixture of Vaseline and benzine. In the next step, the model was surrounded with two cm thick walls made out of modelling clay, so that the distance between the model and the wall was more or less the width of a thumb, to ensure an endurable mold. Where the model touches the modeling clay plate it was lifted a little bit with small hand rolled balls of modeling clay to preserve all features or

to at least allow for enough material, that can be worked with later. For the mold, ELASTOSIL® M 4511 from Wacker Chemie AG a two-component silicone rubber that vulcanizes at room temperature was used. It has a very good flow ability, so it can cover all features of the model precisely. With the addition of a hardening catalyst T 51, the rubber cures on about 8-10 hours without emitting too much heat so that the modelling clay keeps its form. To counteract any deformation during molding process and to make the modelling clay more resistible, it was put in the freezer for 30 minutes at a temperature of about 7 °C. One kg of M4511 was used to cover the whole model in rubber. The rubber is given time over night to cure and was than cut off the cast into two pieces that each cover a caudal or cranial half of the model. The little hand rolled balls of modelling clay were taken out of the silicone rubber form and the holes left will be used as pouring holes for the next step. The rubber mold was cleaned and dried. The inside of the Mold was brushed with a thin layer of marble filler 1000 from AKEMI in jura light with the addition of a hardening paste, to avoid any bubbles. The two halves were put together with the previous bottom part on top and were fixed with cable binders to avoid slipping of the parts. Through the top holes the marble filler 1000, was poured into the form until the fluid reached the top end of the holes. The marble filler cures and hardens in about 30 minutes but to be sure, it was given more time to cure and cool down. When cooled down the model was sanded into its final form. The scapula is 11 cm in length and the coracoid 14 cm.

5.2.3 Remodeling of the scapulacoracoid

The new scapulacorcoid is based on drawings and reconstructions in Wilkinson, M. (2008) of Coloborhynchus robustus (*Anhanguera robustus,* Wellnhofer 1987) and the pictures form Kellner & Tomida (2000). The previously molded cast was used as a basic framework. With the help of modeling clay, the shape of the scapulacoracoid was altered to match the pictures and descriptions seen in Wilkinson, M. (2008) and Kellner & Tomida (2000). The scapula and the coracoid were lengthened. The angle between the scapula and the coracoid was increased a little bit. The biceps tubercle was broadened and rotated laterally. The anterior margin of the scapula was broadened and the transition into the rounded process superior to the glenoid fossa was smoothened. The process itself was made less pronounce and rounded. The glenoid fossa was extended posterior and rotated downward and the superior anterior part of the glenoid fossa was reduced. The tubercle on the posterior flange of the scapula was

made more pronounce. The coracoid part of the glenoid fossa was broadened to created more articular surface laterally. A little tubercle was added to the lateral part of coracoid a few centimeters below the glenoid fossa. The finished model was molded and casted again.

For the mold ELASTOSIL® M 4511 from Wacker Chemie AG was used, which cures with the addition of a hardening catalyst T51 in about 8-10 hours. One kg of M4511 was used. The rubber was given time over night to cure and was then cut off the cast into two pieces. The insight of the Mold was brushed with a thin layer of marbel filler 1000 from AKEMI in jura light with the addition of a hardening paste, to avoid any bubbles. The two halves were put together and fixed with cable binders to avoid slipping of the parts. marble filler 1000 was used to fill the form. The marble filler cures and hardens in about 30 minutes. When cooled down the model was sanded. The scapula is 12 cm in length and the coracoid has a length of 17 cm. The finished model was covered in a thin layer of molding clay, to create a non-reflective surface that was important for the next step, which was, Photogrammetry.

5.3 Photogrammetry and 3D model

Photogrammetry is a method, which allows one to reconstruct the surface features and other properties, such as positioning in space of an object, with the help of pictures. With photogrammetry, one can create three-dimensional coordinate systems, maps, digital geometric models or three-dimensional models (Kraus, Harley & Kyle, 2007). For the picturing process, a freestanding standard size table was used on which a turntable from Crofton was placed right in the middle. On top of the turntable a wooden plate with a length of 80cm and a width of about 50 cm was placed. It was not necessary to fix the plate to the turntable, as the weight of the wood was enough to cause friction high enough so that the turntable and the wooden plate moved as one functional unit. To avoid any shadows thrown by the object, which later could lead to any difficulties in generating the 3d model, 5 table lamps were placed around the wooden plate and adjusted to evenly light the surface. A camera tripod was placed next to the table. A Fujifilm X-T3 camera was used to take photos with a 35mm lens for close ranges. The camera was slightly elevated in relation to the model and 50 cm away from the object. The humerus was placed in the centre of the wooden plate with the humeral head facing towards the camera. A photo was taken and the plate was turned 10° and another one was taken. This procedure was repeated until the humerus

was back in its starting position. The same procedure was done along the length axis. The same was repeated with the scapulacoracoid, the only difference was that the scapulacorcoid started lying on its caudal side and was than rotated onto its cranial side. The images were imported to a software called Agisoft Metashape. Agisoft Metashape is a photogrammetric processing software of digital images and generates 3D models out of imported images (Agisoft, n.d.).

124 pictures of the scapulacoracoid and 104 pictures of the humerus where imported to generated two separate 3D models. The models were exported as an .obj file.

5.4 Wing bone alignment

The positioning of the bones were measured from the drawings of Bennet in his 2007 paper. The angles were determined and transferred to Excel. With the angles and the length of the bones from Tomida & Kellner (2000), the half span could be calculated.

5.5 Wing shape and -area

A pterosaur wing can be simplified as a rectangular triangle. One length of this triangle was given by the half span, as mentioned in the previous method above. The other length is the inner length of the wing. For this project, an ankle attachment of the wing membrane was used. The inner length of the wing was measured from the drawings of the Kellner & Tomida (2000) paper. The bones where measured from the drawing and then compared to the lengths given in this paper to ensure the drawing was drawn proportionally. For the inner length of the wing, the distance between the anterior part of the scapulacoracoid and the ankle was measured and scaled to its original size.

5.6 Software

5.6.1 Blender 2.79

Blender is an open source 3D software used for modeling, animation, rendering, motion tracking, etc. The Software is a free download and easy to use and learn and doesn´t need any supplemental hardware to get a satisfying model. (Blender, n.d)

For this project, the Version 2.79 was used. The .obj data obtained by photogrammetry was imported into Blender. The editing and sculpture mode were used to further

change the model of the humerus and scapulacoracoid according to the pictures of the American Museum of National History (AMNH) for *Anhanguera santanae* (American Museum of National History, 2007). With the help of the applications build into the software the humerus and the scapulacoracoid where resized to fit the measurements of Kellner & Tomida (2000). The missing parts of the wing where modelled to create a 3D model of the left wing of *Anhanguera*. In the next step, muscles where created and attached to the wing with the help of Bennetts' papers from 2007. With the 3D-print tool, the volume of all elements where calculated and exported to Excel. The software was used to obtain the radius of the humerus at its smallest diameter, in the x- and y-axis in its in vivo position. Rendering wasn´t possible because of the lack of computational processing power of the computer the software was ran on.

5.6.2 XFLR5 6.47

XFLR5 is an open source and free to download software. It is a tool to analyze airfoils, wings and planes operating at low Reynold numbers and incorporates the XFoil airfoil design code for an easy direct and inverse analysis and modeling of an airfoil (XFLR5, 2019). The airfoil used for this study was provided by Collin Palmer and analyzed via the XFoil direct analysis. A Type 1 batch foil analysis was applied, in a range of 200 000 to 500 000 Reynolds numbers and an attack angle range of alpha -10° to 20°. After analyzing, the graphs were exported to Windows Excel and the maximum Lift Coefficient (Cl_{max}) values read of the operating point list.

5.6.3 MATLAB

MATLAB from Mathworks is a programming platform with a matrix-based language to find solutions for a given problem quickly. The Software can be used to analyze data, create models, algorithms and applications. The built-in math functions let you calculate simple and complex calculations (MATLAB, 2020). For this Project the online free monthly trail, version R2019b, was used to calculate the area of two functions by integration. Matlab also was used to fit the bell shaped and the elliptic curve to the area of the wing.

5.7 Body mass

The volume obtained with blender for the bones and muscles where used to calculate the mass of the individual parts. The volume of the muscles was multiplied with the density of birds' muscles to obtain the weight of each one. The muscle density was calculated using the data presented by Sullivan, McGechie, Middelton and Holliday (2019). For the weight of the bones, a slightly different approach was used. The volumes of the bones were multiplied with the bone density mentioned by Martin & Palmer (2014). To consider the hollowness of the bones, the weight was than multiplied with an air space proportion factor proposed by Martin, Palmer & Claessens (2014). All weights were then added up together to sum up the weight of the wings and upper body. The weight of the membrane was neglected in this project. With the help of the proportional weight distribution of the different body parts from Henderson mentioned in the supplemental material of Palmer & Dyke (2011) the body weight was calculated.

5.8 Bone stress analysis humerus

The relative failure force was calculated for the smallest diameter of the humerus using a bone stress analysis for bending used in the following papers Naish & Witton, (2017); Mark Witton & Habib (2010); Habib, (2008). The radius in the x and y plane was obtained with the help of Blender 2.79. A wall thickness of 1mm (Martin & Palmer, 2014) was used.

5.9 Lift calculation

For the lift distribution, the approximation process of Otto Schenk (1940) to determine the lift distribution across a wingspan was used. The procedure makes the plausible assumption that the lift distribution lies between the form of the wing and ideal distribution. The ideal distribution with minimal induced drag would be an elliptical one. The wing was separated into eight sections, one section for each bone along the wing half span. The radius and the ulna were put together into one section. The distribution was than calculated for each segment, by integration of the curves function for each segment. Each segments' integrated area were multiplied by C_{Lmax} and $q_{max,}$ to give the lift force in Newton. Furthermore, the local shear force (ql) and overall shear force (Q) were calculated for each section of the wing. The bending moment (Bm) was

calculated using the Q values. The torsion moments are not calculated. Another simpler method also was used to calculate the bending moment. The assumption was made that each wing has to generate the force of half the bodyweight.

5.10Muscle Force calculation

To calculate the force, the pectoral muscle has to generate to hold the wing in a gliding position a simple assumption can be made. The bending moment in the shoulder has to be equal to the lever of the pectoral muscle multiplied with the force it generates. The lever for the muscle was calculated using the simple trigonometric functions. Knowing the force of the pectoral muscle and the angle of its attack, the horizontal and vertical parts of the vector could be calculated, again using simple trigonometric functions. With the help of the surface area of the humeral head and the horizontal force component, the stress acting on that surface was calculated.

Abbreviations:
Kg - Kilogram, °C – degree Celsius, g - gram, mm- Millimeter N- Newton, Nm- Newton meter, N/m^2 – Newton per square meter, Pa- Pascal, MPa- Mega Pascal

6 Results and Discussion

As this project is a biomechanical study of the shoulder and the force generated by the pectoral muscle during gliding flight, the two skeletal parts important for this study are the scapulacoracoid, which is the shoulder blade fused with the coracoid and the upper arm also called the humerus. Those two parts where closely examined to verify the accuracy of the cast used for this project and if it resembles the fossil remains of *Anhanguera blittersdorffi*. After doing some research on the fossil remains of *Anhanguera blittersdorffi* (Campos & Kellner,1985), it became clear that the postcranial parts must have been, either copied from other specimens of Anhangueridae or from other genera to fill in the missing parts.

As mentioned above the scapulacoracoid and the humerus are of great importance in this study, so it is of great significance to assign those parts to the same genus and species to see if they can be used for study without any change.

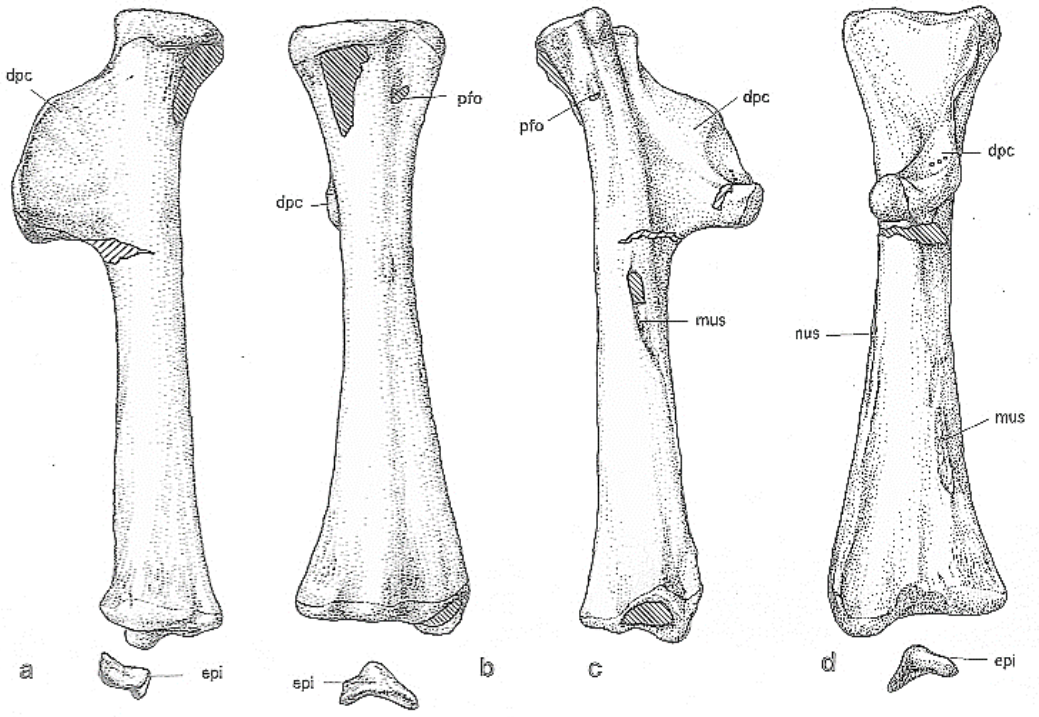

Figure 1: Humerus of *Anhanguera piscator (*Kellner & Tomida, 2000)

The humerus, as can be seen in Figure 1, has a wrapped deltopectoral crest with roughly a third of the shafts length, a kidney shaped convex articular surface and the shaft is ventrally twisted to the humeral head and is therefore typical for an ornithocheiroid pterosaur (Elgin & Frey, 2011)

At a closer look the humerus seems to resemble that of *Anhanguera piscator* (Kellner & Tomida, 2000) or *Anhanguera araripensis* (Wellnhofer, 1985), but in *Anhanguera araripensis* the distal parts of the deltopectoral crest is missing (Kellner & Tomida, 2000). As mentioned by Pinheiro & Rodrigues in their 2017 paper, the species *Anhanguera araripensis*, because of lacking unique features, should be described as a *nomen dubium.* Further, the authors conclude that the morphology of the crest on the premaxilla is size-dependent and mostly not fit as a diagnostic feature for different species of anhanguerid. Excluding those characters reveals that three *Anhanguera* species could count as potentially valid, which are *A. blittersdorffi*, *A. picator* and *A.spielbergi*. They also mention that the postcranial material in some cases does not differ significantly from each other (Pinheiro & Rodrigues, 2017). For those reasons, the humerus will be seen as belonging to the species *A. piscator*.

The scapulacoracoid of the cast doesn´t show any significant resemblance to that of an anhanguerid scapulacoracoid. It wasn´t possible to get any information on, what bones where used to reconstruct the scapulacoraoid. As the scapulacoracoid can not be assigned to any ornithocherid pterosaur, it is necessary to remodel a shoulder girdle that belongs to the same species as the humerus. Therefore, it was necessary to try to reconstruct a scapulacoracoid of an *Anhanguera piscator*. The first model was based on the drawings of Bennett (2008).

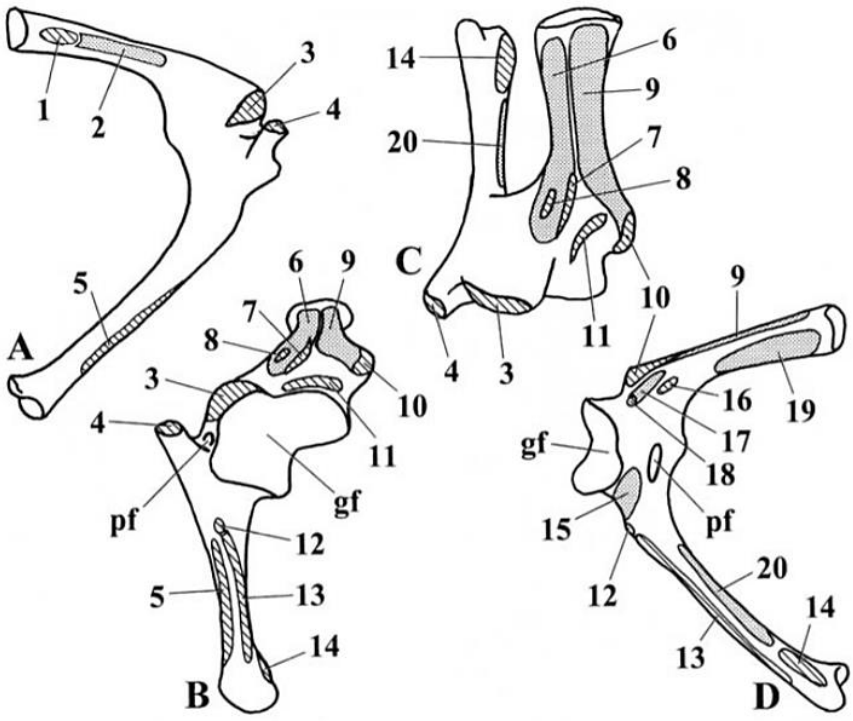

Figure 2: Scapulacoracoid of *Anhanguera* (AMNH 22555). Numbers indicate different muscle attachment points. gf – glenoid fossa, pf – pneumatic foramen (Bennett, 2008)

Figure 3: Scapulacoracoid of *Anhanguera santanae* AMNH 22555. (American Museum of National History, 2007).

The process mentioned in the materials and method was used to reconstruct the shape of the scapulacoracoid. The finished model did not articulate well with the humerus because the pictures in the paper (Bennett, 2008) didn´t show any details of the glenoid fossa and its morphology, as can be seen in Figure 2. The new scapulacorcoid is based on drawings and reconstructions in Wilkinson (2008) of *Coloborhynchus robustus* (*Anhanguera robustus*, Wellnhofer, 1987) and the pictures of Kellner and Tomida (2000) as described above. With the help of those two papers, it was possible to reconstruct the scapulacoracoid more accurately. Using different species of *Anhanguera* to complete the reconstruction shouldn´t be a big issue as the postcranial bones don´t differ too much within Ornithocheirdae. Photogrammetry was used to get 3D models of the Bones. A CT-scan wasn´t used because the bone models wouldn´t show any internal structures and where too big for the departmental micro CT – scanner. The models where then imported into Blender 2.79. The scapulacoracoid was further changed according to pictures of the AMNH (American Museum of National History) of *Anhanguera santanae* specimen AMNH 22555, also suggested by Felipe L. Pinheiro & Taissa Rodrigues (2017) to be pronounced a nomen dubium. The scapulacoracoid of ANHM 22555 can be seen in Figure 3. So the framework was done and an, as far as possible, accurate 3D Model was finished. The situation within the Ornitocheird family is very complicated and highly discussed (Witton, 2013) this work should be representative for a wide range of Ornithocheirdae pterosaurs and should not only be considered for *Anhanguera piscator*. It is more a representation of style of flight. Ornithocheiridae had in general large wings, a small body and seem to have a wing shape similar to seabirds (Witton, 2008). The preferred style of flight seems to have been gliding and soaring long distances (Witton, 2013). This style of flight is what this project focuses on. To calculate the lift of a flying object a few variables must be considered. Firstly, and a very speculative in this case, is the weight of the flying object. In connection to the weight, it is important to mention the gravitational force (G-forces) that act on the plane or animal in flight, which is one in gliding and can increase during curves or during wind

gusts (Kassera, 1991). It is therefore important to know what forces the wings are able to withstand (n_{pos}). In this case it is important to know the relative failure force (RFF) of the bones during flight or easier said how many times the body weight can the bone take in bending stress before breaking (Naish & Witton, 2017). Secondly, the dimensions of the wings and the shape of the wings´ airfoil and how much lift it was able to generate. Also important to flight is the relation of air velocity and air pressure. After Bernoullis´ principal the air pressure lowers at higher speeds and that is the basic principal of how the shape of an airfoil generates lift. Lift is the force, which opposes the inertia of the flying object and is therefore a mayor aerodynamic force (Abbott, Willits & Kailey, 1993). The density of the air, for various calculations used on this study was set to 1,225 kg/m3 at 1013.25 hPa and 15°C at 0 height (Georgantopoulous & Georgantopoulos, 2018).

6.1 Flight muscles

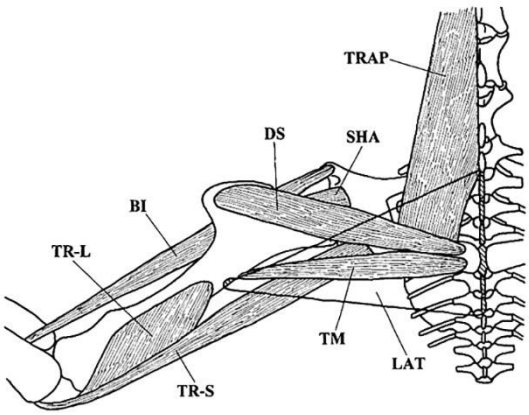

Figure 4: Dorsal view of the shoulder and upper arm**.** TRAP – *m. trapezius,* SHA – *m. scapulohumeralis anterior*, LAT - *m. latissimus dorsi*, TM – *m. teres major*, DS – *m. deltoides scapularis*, BI – *m. biceps*, TR-L – lateral head of *m. triceps*, TR-S – scapular head of *m. triceps*. (Bennett, 2008**)**

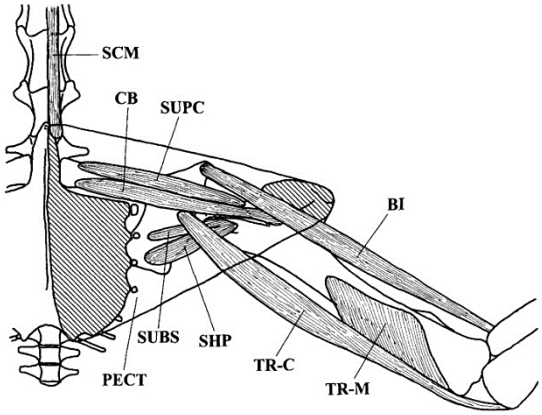

Figure 5: Ventral view of the shoulder and upper arm. SCM – *m. sternocleidomastoideus*, CB – *m. coracobrachialis*, SUPC – *m. supracoracoideus*, PECT – *m. pectoralis*, SUBS – *m. subscapularis*, SHP – *m. scapulohumeralis posterior*, BI – m. biceps, TR-C – coracoid head of *m. triceps*, TR-M – medial head of *m. triceps*. (Bennett, 2008)

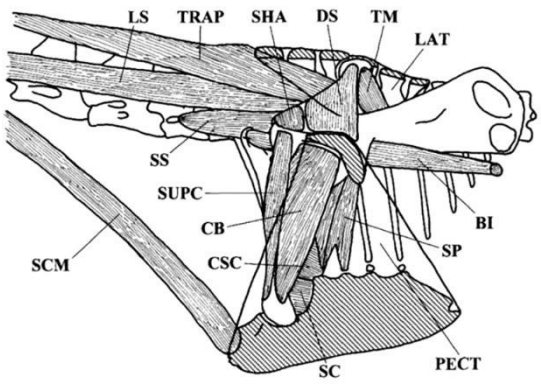

Figure 6: Lateral view of the shoulder. SCM - *m. sternocleidomastoideus*, LS – *m. levator scapulae*, TRAP - *m. trapezius*, SHA - *m. scapulohumeralis anterior*, DS - m. deltoides scapularis, TM - *m. teres major*, LAT - *m. latissimus dorsi*, SS – *m. serratus superficialis*, SUPC - *m. supracoracoideus*, CB - *m. coracobrachialis*, CSC – *m. costosternocoracoideus*, SP – *m. serratus profundus*, SC – *m. sternocoracoideus*, PECT – *m. pectoralis*, BI – m. biceps(Bennett, 2008)

By using the pictures in Bennett 2003, Figures 4 – 6, of the pectoral region of *Anhanguera*, the following shoulder mucles were identified to be the most important in flight*: m. pectoralis, m. coracoideus, m. deltoideus, m. latissimus dorsi, m. supracoracoideus, m. scapulohumeralis, m. triceps major*. It is obvious that *m. pectoralis* would have played the most important role in flapping the wing, producing a force much larger than the other muscles.

6.2 M. pectoralis inclination angle

With simple trigonometry and the measurements from Bennetts' drawings, it was possible to determine the angle of the humerus. To calculate an angle, at least two

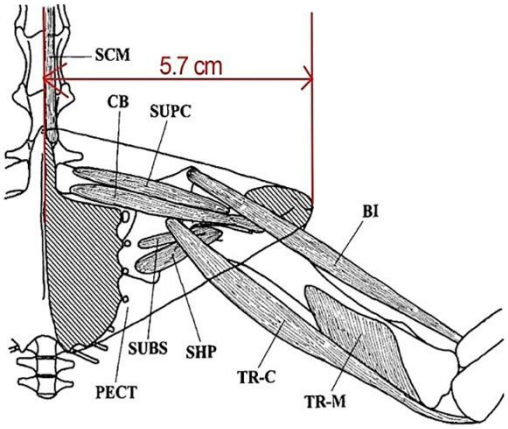

Figure 7: Length of the pectoral muscle in ventral view**.** SCM – *m. sternocleidomastoideus*, CB – *m. coracobrachialis*, SUPC – *m. supracoracoideus*, PECT – *m. pectoralis*, SUBS – *m. subscapularis*, SHP – *m. scapulohumeralis posterior*, BI – m. biceps, TR-C – coracoid head of *m. triceps*, TR-M – medial head of *m. triceps*. (Bennett, 2008)

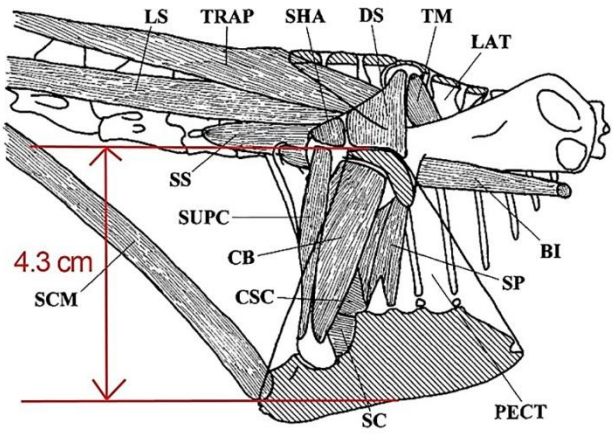

Figure 8: Length of the pectoral muscle in lateral view. SCM - *m. sternocleidomastoideus*, LS – *m. levator scapulae*, TRAP - *m. trapezius*, SHA - *m. scapulohumeralis anterior*, DS - m. deltoides scapularis, TM - *m. teres major*, LAT - *m. latissimus dorsi*, SS – *m. serratus superficialis*, SUPC - *m. supracoracoideus*, CB - *m. coracobrachialis*, CSC – *m. costosternocoracoideus*, SP – *m. serratus profundus*, SC – *m. sternocoracoideus*, PECT – *m. pectoralis*, BI – m. biceps (Bennett, 2008)

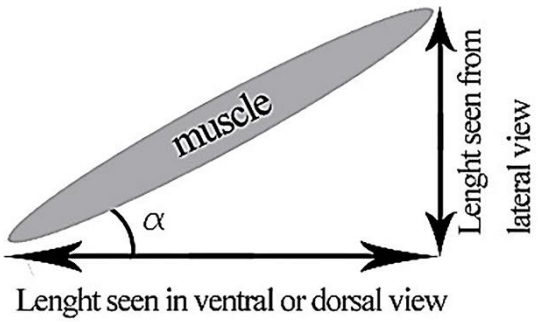

$$\alpha = tan^{-1}\left(\frac{4.3}{5.7}\right) = 37°$$

Figure 9: Relationship of lengths to find the vertical angle

perspectives of the same muscles are needed, for example the lateral, ventral and dorsal view. Using the pictures in Bennett (2003), the length of the pectoralis was measured from two perspectives: the ventral as seen in Figure 7 and the lateral as seen in Figure 8. After the two lengths were measured, the vertical angle of inclination could be calculated using the relationship in Figure 9. To calculate the angle at which the pectoralis force is acting with respect to the humerus, the same pictures were used. The results in Figure 9 represent the *m. pectoralis'* inclination with respect to the vertical and horizontal axis. In order to find out its vertical inclination with respect to the humerus, the inclination of the humerus itself must be taken into consideration. Using the same method as above, the humerus has a vertical inclination of 9°.This means that the pectoralis' vertical inclination with respect to the humerus is 37° – 9° = 28°.

6.3 Wingspan

To determine the dimensions of the wings the bone lengths from Kellner and Tomida (2000) were used and the missing bones were filled into the 3D model. Kellner and Tomida (2000) is a good source as it contains complete measurements of the scapulacoracoid, humerus, radius, ulna and wm4. Also big parts of the fourth wing finger are preserved in their described specimen. The lengths for all digits were measured from the papers drawings, but first it was ensured that the drawing represented all bones proportional. All lengths can be seen in Table 1.

In order to calculate the total wingspan, the length of all the wing bones is needed. The picture below from Wilkinson (Figure 10) shows all the bones needed. However, the wingspan is not only the sum of all the bones' lengths.This happens because all the bones have an inclination with respect to the horizontal axis, which is observed from the dorsal perspective. The Humerus has an inclination of 34 degrees, while the ulna is inclined with an angle of 22 degrees. When looking at the pictures in Bennet (2003) the wing metacarpale has just a small inclination of about 3°.

Table 1: Shows the bone lengths that make up the wing

ulna	390	mm
humerus	255	mm
wm	253,5	mm
wf1	604,5	mm
wf2	546	mm
wf3	409,5	mm
wf4	331,5	mm
scapula	112	mm

The falangs are inclined with an angle of 15 degrees. The total wing span is equal to : wingspan= h * cos(34) + u * cos(22) + wm * cos(3) + (wf1 + wf2 + wf3 + wf4) * cos(15) + sc: where h – humerus length, u – ulna length, wm – wing metacarpals length, wp – wing falangs length, sc – scapula length

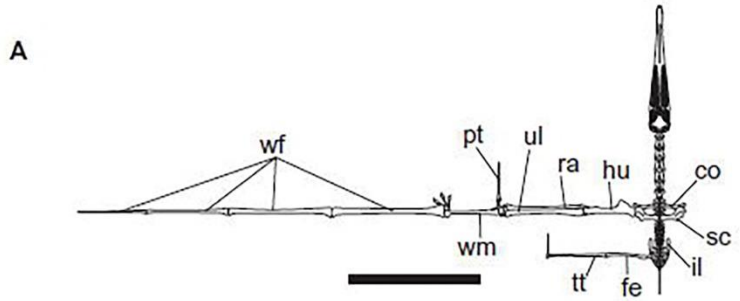

Figure 10: Wing bones of *Anhanguera*. tt - tibotarsus, fe - femur, il - ilium, sc - scapulacoracoid, co - coracoid, hu - humerus, ra - radius, ul - ulna, pt - pteroid, wm – wing metacarpal, wf – wing finger. (Wilkinson, 2008)

6.4 Wingarea and Membrane attachment

The area of the wing is also dependent on the inner length of the wing and in this case where the membrane attaches to the body. There has been a lot of discussions on wether the wing membrane attached to the hip or to the ankle. In earlier pterosaurs such as *Rhamphorhynchus*, there is clear fossil evidence of an ankle attachment. In pterodacytloids the situtation is not quiet as clear, unfortunatly (Unwin, 2006). For this study an ankle attachment was used. The drawings in Kellner & Tomida (2000) were

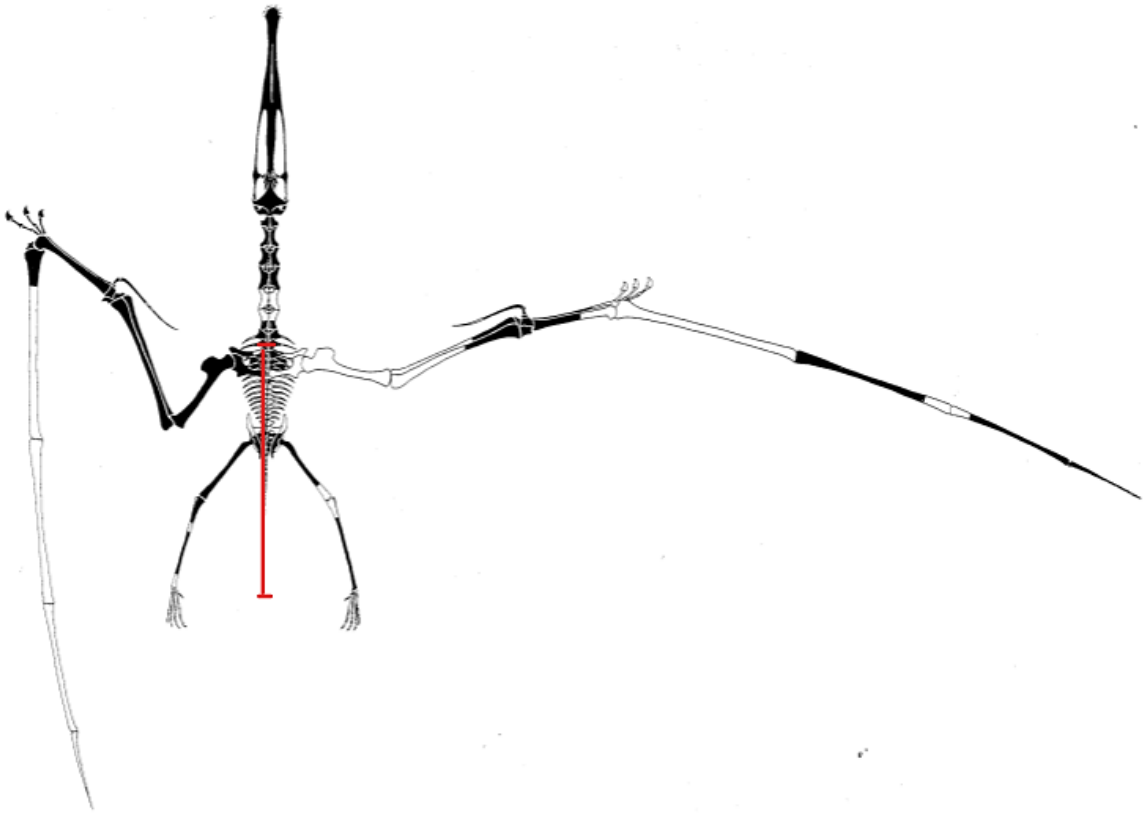

Figure 11: Shows in red the measured distance for the inner cord length. (changed from Kellner & Tomida, 2000)

used to measure the length between the anterior margin of the scapulacoracoid and the ankles. For this model the pteroid bone would not point forward (Unwin, 2006), but medialy towards the shoulder.

Depending on the angles between the scapulacoracoid and humerus and the humerus and the ulna, the propatagium (small membrane between the humerus and ulna) originates more towards the head or the scapulacoracoid. Following the drawings of Bennet (2003, 2008) the propatagium would insert near the scapulacoracoid when pointing medialy in an 22° angle. After measuring, the inner chord length was 790mm form the drawings of Kellner & Tomida (2000) seen in Figure 11. Other Authors also suggested different wingpositions, for example a forward sweep that would change the center of pressure and may stabelise flight (Palmer & Dyke, 2011), but this is not part of this work.

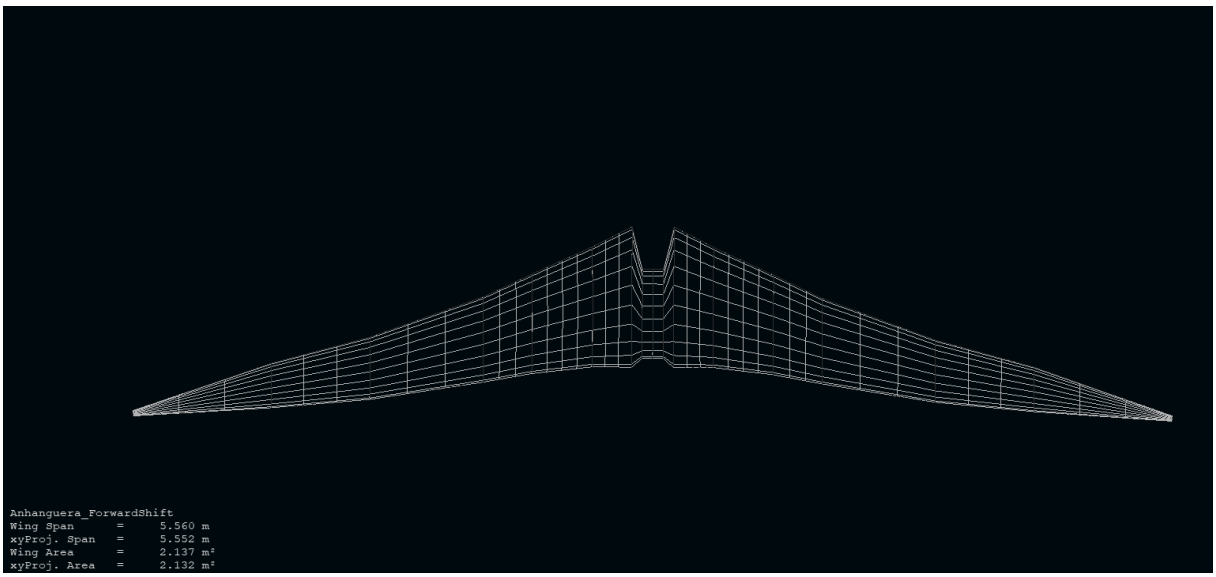

Figure 12: Wing modeled in XFLR5

With the wingspan and the inner chord length known it is now possible to calculate the wing area. Looking at the wingshape of different pterosaur they are almost always reconstructed as triangular shaped wings. To simplify calcultions it is important to also simplify shapes to a certain extant. Therefore the wing will be seen as a simple triangle. So with the standard formula (a * b) /2 the wingarea can be calculated where a is the halfwingspan and b is the inner chord length. The area of one wing is 1,10136342 m^2 and multiplied by two gives you the whole wing area of 2,20142682 m^2. To see wheter that estimation was accurate enough a 3D wing model was created with the software XFLR5, seen in Figure 12. Using the same measurments as mentioned above the wing area was calculated to be 2,137m^2.

6.5 Lift coefficient (Clmax)

The lift, a wing can produce is not only dependent on its wingspan and –area but on the shape of the airfoil. There are no direct analogues in today's world to a pterosaur wing other than maybe a bat, but the diameter of bats bones are much smaller in correlation to the chord length of the wing (Palmer; 2015). It is hard to reconstruct the membrane of a pterosaur because of lack of fossils with preserved tissue as mentioned before. This is, for those reasons a highly speculative topic and I lean therefore on the PhD thesis of Collin Palmer (Palmer, 2015). He was so kind to share his used wing foil files with me.

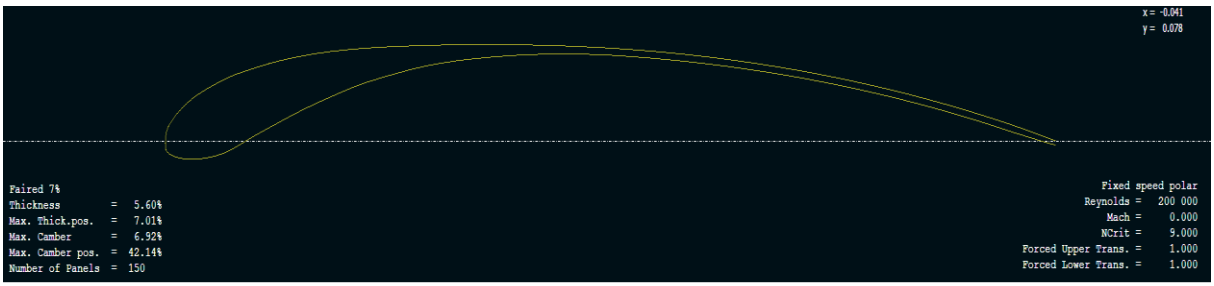

Figure 13: Airfoil used for the Batch Analysis

The airfoil seen in Figure 13, was used for the whole wing and does not differ on each section of the wing. Other shapes can be possible but should be subject of other studies. To obtain the Cl_{max} values, a Type 1 Batch Analysis, was run with this airfoil at Reynolds numbers ranging from 200.000 to 500.000 and angle of attack (alpha) values of -10° to 15° at increments of 0,500. This type of Batch analysis gives the equivalent results of a standard wind tunnel test.

The Reynolds number is a dimensionless number to describe the ratio of inertial forces to viscous forces and can be used to show in which fluid systems the viscosity has an important controlling factor of flow velocities. At low Reynolds numbers the flow is dominated by a laminar flow and at high numbers by a turbulent flow. Pterosaurs are assumed to have flown at low Reynolds numbers of 200.000 to 500.000 (Palmer, 2015).

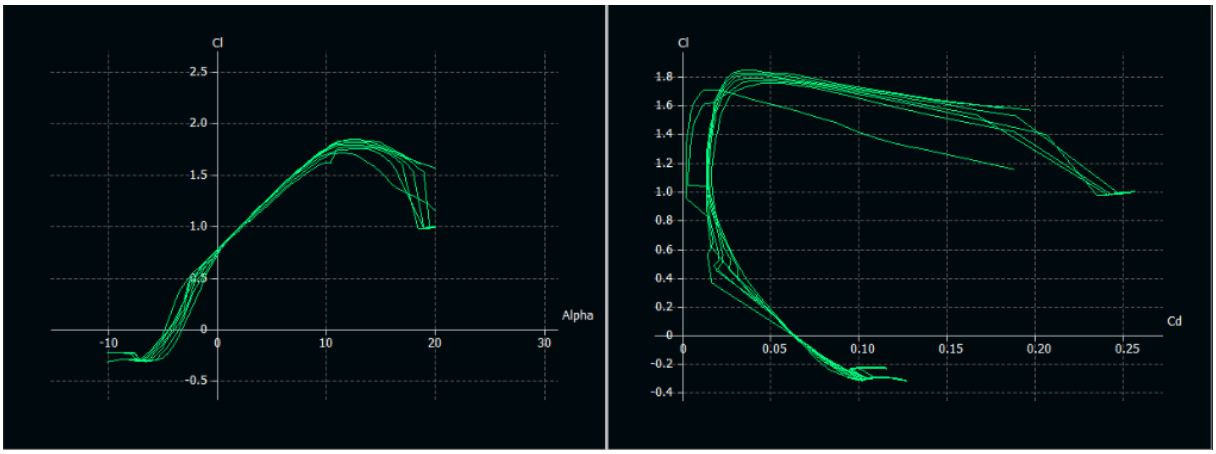

Figure 14: Resulting graphs of Batch Analysis. Alpha – angle of attack, Cl – lift coefficient, Cd – drag coefficient

The resulting graphs of the batch analysis were evaluated and the highest possible lift coefficient was isolated. As seen in Figure 14 the highest possible Cl occurs at an angle of attack of 12,5° and has a value of 1,85. This value is near the absolute maximum measured in modern birds under steady conditions (Witton & Habib, 2010). As mentioned before there are many other possible airfoil profiles and

Clmax values, which one is the closest to a living pterosaur is subject to future studies and not part of his project. At a Cl_{max} of 1,85 the airfoil has a drag coefficient (Cd) of 0,032. The glide angle can now be calculated using the following expression: tan α = Cd/Cl. At Cl_{max} the glide angle is 1,553° or in other words for every meter the pterosaur would lose in height it would travel 57,81 (1 : 57,81) meters. The optimal glide angel is at the highest Cl/Cd (Cl = 1,592 / Cd = 0,017) values and would lead to a glide ratio of 1 : 93,65. The fastest glide angle would be at the lowest drag values (Cl = 1,2 / Cd = 0,013) and would mean a travel of 92,30 meters for every lost meter in height (Kühr, 1996; Kassera, 1991).

6.6 Body mass

Body mass is an important parameter in the life of flying animals and effects the speed in flight and maneuverability as only two examples of many more. The body mass also sets a limit on the capability of flight. (Martin & Palmer, 2014). For those reason it is very important to find a lifelike estimation of the weight of pterosaurs, which is hard to do. Pterosaur have been compared to birds many times in the way they flew or took off, but recent studies have shown, that the flying reptiles would struggle with those strategies. (Witton & Habib 2010). The main methods used to estimate mass are, the estimation of total body volume and the distribution of densities or the relationship of skeletal mass and total mass (Martin & Palmer, 2014a). The mass estimations for this work is a combination of different methods. To calculate the dry bone mass of the wing bones, the volumes of the reconstructed bones where obtained with the 3D print tool in Blender 2.79. The volume is then multiplied with the density of pterosaur bones which is estimated to be 2,05 g/cm^3 (Martin & Palmer, 2014). The bone would be completely filled with bone mass and would not have any air in it, but as pterosaur bones are highly pneumatized it is important to account for the amount of air within the bone. The study by Martin, Palmer & Claessen (2014) was used to multiply the results with an Air Space Proportion (ASP) factor for each wing bone, seen in Table 2 . The outcomes from this approach were compared to the masses mentioned by Martin and Plamer (2014) in their supplemental material for the Wf1. Their Soton Wf1 has a length of 570 mm, weighed 117,6 g whereas the Wf1 used in this study has a length of 604 mm, and weighed 126,48 g. The values calculated seem not to be far off using the ASP method and one can be satisfied with the outcome. It has to be stated that the

ASP could vary in different pterosaurs, as the study by Martin Palmer & Claessen (2014) mainly looked at Ornithocheiridae bones.

Table 2: Air Space Proportion and the weight for every wing bone.

ASP (Air Space Proportion)		Bone weight	
humerus	0,9	57,98	g
ulna	0,81	91,14	g
radius	0,9	16,12	g
wm4	0,86	53,78	g
wf1	0,81	126,48	g
wf2	0,76	56,43	g
wf3	0,68	40,46	g
wf4	0,6	16,54	g
scapulacoracoid	0,81	52,51	g

It would have been a possibility to repeat this process for every bone of the body to get the total dry bone mass and then the body mass via their relationship as mentioned before. There wasn´t a scanner available big enough to scan the whole pterosaur cast, so another method was used. With the help of the Bennett papers from 2003 and 2008 one was able to reconstruct the most important muscles in the wing and upper body using Blender 2.79. All muscles were placed at the exact points of origin as described in the papers. The size of each muscle is highly speculative but was modeled to not exceed those in the drawings of Bennett (2003, 2008). There is of course a difference, because the drawings are in 2D and giving them a third dimension can change the volume and therefore the weight significantly. All muscles are scaled proportionally to their drawn counterparts, so that smaller muscles are not overinflated in volume. All muscles reconstructed are mentioned in Table 3. With the 3D print tool of Blender 2.79 it is possible to obtain the volumes of all muscles. To calculate the mass of each individual muscle, it is necessary to know the density of the muscles.

To tackle this issue it is important to look at where Pterosauria are rooted in the three of life. Pterosaurs are Vertebrata and because they possess four well-developed limbs, belong to a clade called Tetrapoda. Their skeletal anatomy also shows, that they could lay their eggs outside of the water, which moves them into the clade of Amniota. Pterosauria are therefore either mammals, reptiles or birds. Some distinct features in their anatomy and bones structure point towards a reptilian descent (Witton, 2013).

Table 3: All reconstructed muscles

m. latissimus dorsi	*m. triceps coracoid*
m. pectoralis	*m. triceps lateral*
m. trapezius	*m. triceps medial*
m. coracobrachialis	*m. triceps scapular*
m. subscapularis	*m. extensor carpi radialis*
m. supracoracoideus	*m. extensor carpi ulnaris*
m. levator scapulae	*m. extensor digiti longus*
m. serratus profundus	*m. flecor carpi radialis*
m. bizeps	*m. flexor digitorum longus*
m. brachialis	*m. flexor digitorum longus* ulnar head
m. deltoideus scapularis	*m. flexorcarpi ulnaris*
m. humeroradialis	*m. pronator teres*
m. scapulohumeralis anterior	*m. supinator*
m. scapulohumeralis posterior	*m. extensor digiti quarti brevis*
m. teres major	*m. flexor digitorum brevis*

Where exactly their origin lies within the reptiles is not yet fully resolved but the current notion is, that together with dinosaurs they are put into a group called Ornithodira, which would also make them true Archosaurs (Witton, 2013). Unwin (2005) also mentioned another possibility where pterosaur originated lower in the diapsid tree, putting them in a group called Archosauriformes. To sum up this brief excursion it can be stated that pterosaurs are closer related to crocodiles and birds than to mammals. crocodiles and birds should therefore give us a good insight into the properties of their soft-tissue (Witton, 2013).

The density of archosaur skeletal muscle is 1,056 g/cm^3 (Gignac, & Erickson, 2016) and that of a bird like the European Starling (*Sturnus vulgaris*) is about 1,055 g/cm^3 (Sullivan, McGechie, Middelton & Holliday, 2019). For this study, the density of 1,055 g/cm^3 was chosen to calculate the muscle mass as it should not make a big difference when calculating with the lower value as it only differs one thousandth of a gram. The weight for each muscle was calculated using the following scheme: mass = volume * density. All muscle masses were than assigned to a section on the wing. The sections on the wing are the lengths of the bones on the y-axis. This gives the same

sections, as mentioned in a previous chapter, which were used for calculating the wingspan. The sections are seen in Table 4.

Table 4: Shows all bone lengths, as they would be represented on the y-axis and the end of each section on that same axis.

Wing span sections	***Bone lenght on y-axis***		***End of Section on y-axis***	
scapulacoracoid	112	mm	112	mm
humerus	213,86	mm	325,86	mm
ulna	361,60	mm	687,46	mm
wm	253,15	mm	940,61	mm
wf1	604,5	mm	1545,11	mm
wf2	527,39	mm	2072,51	mm
wf3	395,54	mm	2468,05	mm
wf4	320,20	mm	2788,26	mm

Table 5: Shows volumes of selected bones and muscles and the calculated masses summed up for the humeral and scapulacoracoid section.

	Volume (cm^3)		**Volume (cm^3)**
humerus	282,85	**scapulacoracoid**	134,82
m. bizeps	67,17	*m.deltoideus scapularis (1/4)*	12,965
m. brachialis	27,13	*m. scapulohumeralis anterior (1/2)*	1,95
m.deltoideus scapularis (3/4)	38,89	*m. scapulohumeralis posterior (3/4)*	4,05
m. humeroradialis	29,85	*m. teres major (1/2)*	14,66
m. scapulohumeralis anterior (1/2)	1,95	*m. latissimus dorsi*	199,04
m.scapulohumeralis posterior (1/4)	1,35	*m. pectoralis*	2598,72
m. teres major (1/2)	14,66	*m. trapezius*	117,54
m. triceps coracoid	133,01	*m. coracobrachialis*	9,42
m. triceps lateral	45,43	*m. subscapularis*	4,22
m. triceps medial	39,26	*m. supracoracoideus*	9,87
m. triceps scapular	123,10	*m. levator scapulae*	98,25
		m. serratus profundus	30,88
Muscle Mass	550,50 g	Muscle Mass	3272,16 g
Bone Mass	57,98 g	Bone Mass	52,51 g

If a muscle lies in two sections the volume of the muscle was divided by how much of the muscle lies in each section, as seen in Table 5. For example, *the m. scapulohumeralis anterior* lies almost central between the scapulacoracoid and the humerus und therefore one half of the volume was assigned to each section. As can

be seen above the pectoral muscle was fully assigned to the scapulacoracoid section, which actually is the body itself.

After adding up all bone and muscle masses in their section, the sum of all sections, excluding the scapulacoracoid, gives the weight of the wing. With the help of the proportional weight distribution of the different body parts mentioned in the supplemental material of Palmer & Dyke (2011) the body weight was calculated. The percentile distribution of different authors can be seen in Table 6.

Table 6: Mass of body parts in percentage total.

	B&W	**Henderson**	**Strang**
Head	5,2	12,0	6,1
Neck	4,9	4,0	6,1
Body	52,4	55,0	36,3
Legs	5,0	5,0	7,9
Wings	32,5	24,0	43,6

The weight of each arm came up to 2018,51 g. The body weight was calculated for all three authors' suggestions. All results are shown in Table 7 below.

Table 7: Masses calculated using the different weight distributions.

	Henderson	**Strang**	**B&W**
Total	16820,88 g	9259,20 g	12421,58 g
Wing	4037,01 g	4037,01 g	4037,01 g
Body	9251,48 g	3361,09 g	6508,91 g
Neck	672,83 g	564,81 g	608,65 g
Head	2018,50 g	564,81 g	645,92 g
Legs	841,04 g	731,47 g	621,08 g

All three results can be considered low for an individual with a wingspan of 5,5 meters compared to Witton (2008) or Palmer & Dyke (2010). For choosing one of the three results, the scapulacoraoid section was taken into account, as it actually represents the complete upper body. The weight of the left and right scapulacoracoid sector combined is 6649,363 g. This would rule out Strangs and Bramwell & Whitfields prediction as in their scenario the body must have been lighter. For this reason the mass estimation following Strangs` mass allocation was used going forward and will

be the inertia for this studies pterosaur. For the following bone stress analysis, this weight and the weight calculated following Palmer & Dyke (2010) were used to estimate the RFF in bending of the humerus.

6.7 Bone stress analysis

During flight, there are tremendous forces acting on the bones and muscles but when the structure is overloaded and fails to withstand those forces. The bones of many Ornithocheiridae pterosaurs are very thin walled structures that can bear a decent amount of stress as this analysis will show later. The humerus is essentially a hollow tube with an elliptical cross section at its smallest cross section underneath the deltopectoral crest. A simple beam model was applied to calculate the maximum stress in bending, in both the sagittal and coronal plane (Naish & Witton, 2017; Witton & Habib, 2010; Habib, 2008). To calculate the second moment of area, the section modulus and the maximum stress, the diameter in which the bending occurs, the wall thickness and the bone length have to be known. The radii were measured from a dorsal or ventral point of view and a posterior or anterior point of view with the help of Blender 2.79. A wall thickness of 1mm, which is an average of the data published in Martins & Palmers paper 2014, was used. To calculate the second moment of area (I) the following formula was used:

$$I = \pi \,/\, 4 \left(R_1 R_2^3 - R_3 R_4^3 \right)$$

R1 and R2 are the total bone radii and R3 and R4 are the radii of the bone cavity or R1 an R2 minus the wall thickness (Naish & Witton 2017). The section modulus (Z) is the second moment of area (I) divided by the maximum distance (y) from the neutral point to the outer edge of that section.

$$Z = \mathrm{I/y}$$

The maximum stress was calculated using the following formula:

$$\sigma = WL \,/\, Z$$

where W is the weight loaded onto the structure in Newton, L is the bone length in mm and Z is the section modulus. To calculate the relative failure force for the humerus the breaking limit of the bones had to be assumed. Authors like Naish & Witton (2017) and Witton & Habib (2010) assumed those values to be 162 Mpa and 175 Mpa respectively. Both values were taken into consideration and used for the bone strength analysis.

Table 8 shows the values used and the results for an animal with a body weight of 16,8 kg at a breaking limit of 162 Mpa and 175 Mpa. Underneath the same results are shown for an animal with a body weight of 34,70 kg, following the mass calculation of Palmer & Dyke (2010).

Table 8: Variables and results of the stress analysis of the humerus

		sagittal bending	**coronal bending**
total bone radius sagittal	R2	14	15,25
wall thickness	th	1	1
inner bone radius sagittal	R4	13	14,25
total bone radius coronal	R1	15,25	14
inner bone radius coronal	R3	14,25	13
second moment area	I	8277,11	9452,08
section modulus	Z	591,22	619,814
maximum stress (Mpa) (16,8kg)		71,17	67,89
RFF (16,8kg) 162 Mpa		2,27	2,39
RFF (16,8kg) 175 Mpa		2,45	2,57
maximum stress (Mpa) (34,70kg)		146,83	140,06
RFF (34,70kg) 162 Mpa		1,10	1,156
RFF (34,70kg) 175 Mpa		1,19	1,25

The results show that the humerus could withstand a decent amount of stress with more than two times the body weight at 16,8 kg. With breaking limits at 162 Mpa the bone would withstand a body weight of 38,28 kg before buckling under its own weight because the RFF would sink under one. At breaking limits of 175 Mpa a body weight of 41,35 kg would be possible. It has to be stated that in order to glide at steady conditions each humerus would only have to withstand the forces of half the body weight, which means that the maximum body weight could be higher. The RFF is nevertheless a good proxy, because it is easy to compare the strength of the bones to other publications that use the same method and therefore will be used in this study as the maximum amount the bone can withstand.

Those results show that the pterosaur used in this study would be able to glide at a weight of 38,28 kg to 41,35 kg at steady conditions but would not leave any room to balance out any disturbances that arise during flight. With that weight, it would not

be possible to flap or fly any curves, which does not seem likely for a living animal, as it must be able to offset changing conditions in the air such as wind gusts. Those numbers are very low considering that modern birds experience 10 – 14 G-forces routinely during flight. (Simons, 2009; University of Michigan, 2008)

As mentioned above the RFF will serve as the maximum G-forces that can be withstood during gliding, which means the maximum n_{pos} will be one for steady gliding, 2,33 (mean of 165 MPa breaking limit) and 2,52 (mean of 175 MPa breaking limit) for non-steady conditions.

6.8 Lift Distribution and Calculation

To calculate the forces that act on the shoulder, it is important to look at how lift is distributed along the wing during gliding. For an aircraft the ideal distribution is ellipse shaped, because it produces the lowest numbers of induced drag (Kassera, 1991) and has become, since it´s publication in 1922 by Prandtl the standard design tool in aviation (Eslinger, Murillo, Jensen, Gelzer & Bowser, 2016). That is why many fighter aircrafts in the Second World War had elliptical shaped wings but any deviation from this shape results in induced drag (Palmer, 2015.) In 1933, Prandtl published a new paper and presented a more efficient span load called the bell-shaped distribution. In 1935 Reimar Horton also published a bell shaped wing loading. This bell-shaped wing loading distribution also applies for birds and most likely for pterosaurs as well, as their wingtips are long, small and light and won´t support the load as good as the short large and heavy wingtips of an aircraft (Eslinger, Murillo, Jensen, Gelzer & Bowser, 2016). To calculate the lift distribution an approximation process by Otto Schenk (1940) was used. Otto Schenk makes the plausible assumption that the real lift distribution (t_{Schenk}) is a mix between wing shape and the optimal lift distribution. In this study the wing shape was simplified to a triangle (t_{Wing}) and both the elliptical (t_{Ell}) and the bell shape (t_{Bell}) span load were used. The area underneath each curve has to be equal to the wing area. The real lift distribution is the difference between the triangle and the shape used for the span load. If transferred to a coordinate system the wing and the span loads would have the following expression, mentioned in Table 9.

Table 9: Expressions used to calculate the area for each distribution and the wing.

t_{wing}	0.2832 * x +0.79
t_{Ell}	0.5028 * sqrt(1 - (x/2.788)^2)
t_{Bell}	0.86435 - (0.938 * x / 2.788)^2)^2

To get the real lift distribution the following formulas were used:

$t_{SchenkEll} = (t_{wing} + t_{Ell}) /2$

$t_{Schenk\ Bell} = (t_{wing} + t_{Bell}) /2$

MATLAB was used to calculate t_{Schenk} and the Figures 15 and 16 show the resulting span loads.

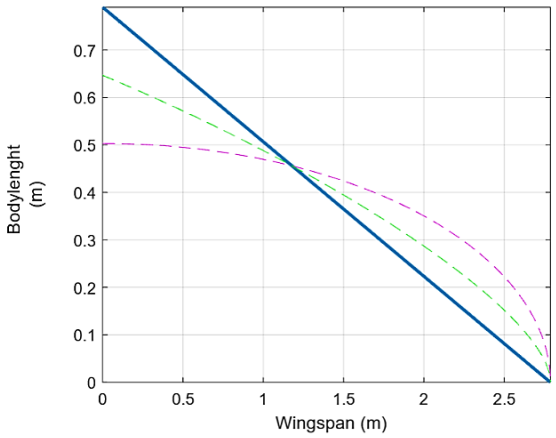

Figure 15: Elliptical lift distribution. Graph shows the elliptical lift distribution (pink) the triangular wing (blue) and their cross product (green)

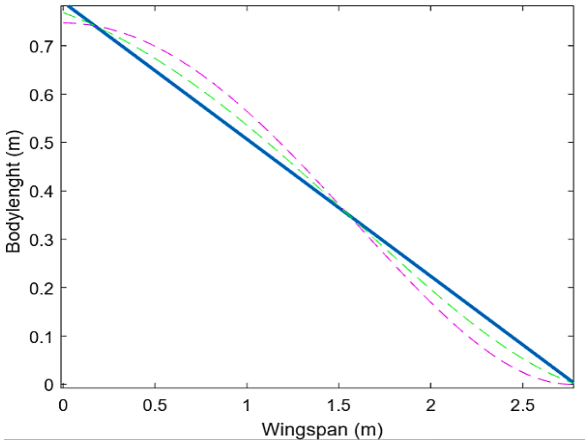

Figure 16: Bell shaped lift distribution. Graph shows the bell shaped lift distribution (pink) the triangular wing (blue) and their cross product (green)

The distribution values were calculated by integrating the t_{schenk} for each scenario. For the boundaries, the y values of the eight wing sections as mentioned in a previous chapter were used.

To get the lift force for each segment the span load values had to be multiplied with the maximum dynamic pressure (q_{max}) acting on that segment and the Cl_{max} value. For this study, the Cl_{max} is the same for each segment but would most definitely be different in nature.

First, the maximum allowed weight force was calculated using: $F_{Gmax} = m*g*n_{pos}$ (M. Milkovits, 2020, pers. comm., 22 January). The dynamic pressure was calculated with the following formula: $q_{max} = F_{Gmax}/ (C_{Lmax}*A_{wings})$ (M. Milkovits, 2020, pers. comm., 22 January), were A_{wings} is the area of the wing. With the addition of the air pressure (ρ) the maximum velocity (v_{max}), the stall speed (v_s) and the maneuver speed in horizontal flight (v_a) were calculated using the formulas seen below:

vmax $\sqrt{(2*q_{max}/\rho)}$

vs $\sqrt{(2*m*g/Cl*S*\rho)}$

va $vs*\sqrt{n_{pos}}$.

Table 10 shows the results for n_{pos}, also called G-forces of 1 and 2,3 and 2,52 in gliding. This pterosaur would have been able to glide at speeds of over 29 km/h up to 44,69 km/h at G-forces of 2,3 and up to 46,45 km/h at 2,52 G and would stall at anything below the 29 km/h mark (M. Milkovits, 2020, pers. comm., 22 January).

Table 10: Calculated speeds under different conditions of loading.

	n_{pos} 1				**n_{pos} 2,3**				**n_{pos} 2,52**			
F_{GMax}	165,01	N			384,68	N			415,55	N		
q_{Max}	40,49	Pa			94,40	Pa			101,97	Pa		
v_{Max}	8,13	m/s	29,27	km/h	12,41	m/s	44,69	km/h	12,90	m/s	46,450	km/h
v_S	8,13	m/s	29,27	km/h	8,13	m/s	29,27	km/h	8,130	m/s	29,27	km/h
v_A	8,13	m/s	29,27	km/h	12,41	m/s	44,69	km/h	12,90	m/s	46,45	km/h

The lift for each segment was calculated using the following expression:

$$L = \mathrm{Clmax} * \mathrm{qmax} * \int_a^b tSch\,(x) * dx$$

where L is the lift in N and a and b are the boundaries of the segments to be calculated (M. Milkovits, 2020, pers. comm., 22 January). The force that counters the lift is the inertia of the wing and therefore must be subtracted from the lift values to calculate the local shear force (ql). This was again done for every of the eight wing segments and only describes the local shear force without accounting for the forces of the previous sections. We can not only look at the sections separately but also have to take into consideration that forces and moments carry on span wise. The sum of ql will be called

Q (overall shear force). At the wing tip, only the force of the most outside segment has to be taken into consideration, that is why q and Q have the same value in the most outside segment. The next inside section is loaded with local force and the force of the previous segment. This was repeated until the last segment at the wing root was calculated. The local and overall shear forces were calculated at the middle of every segment.

Table 11: All results of the lift distribution and bending moment under steady gliding conditions.

Wing Section	Lift (L)	Inertia	local Shear Force (q)	Shear Force (Q)		Qpoints calculated		Biegemoment (Bm)	
scapula coracoid									
$t_{SchenkEll}$	5,36	62,70	- 57,35	0,00	N	0,056	m	72,98	Nm
$t_{Schenk\ Bell}$	6,38	62,70	- 56,33	0,01	N	0,056	m	60,11	Nm
humerus									
$t_{SchenkEll}$	9,84	5,97	3,87	57,35	N	0,218	m	63,63	Nm
$t_{Schenk\ Bell}$	11,73	5,97	5,76	56,34	N	0,218	m	50,93	Nm
ulna, radius									
$t_{SchenkEll}$	15,45	10,11	5,33	53,48	N	0,506	m	48,25	Nm
$t_{Schenk\ Bell}$	18,18	10,11	8,07	50,58	N	0,506	m	36,38	Nm
wm 4									
$t_{SchenkEll}$	9,87	1,37	8,50	48,14	N	0,814	m	33,45	Nm
$t_{Schenk\ Bell}$	11,21	1,37	9,84	42,51	N	0,814	m	23,31	Nm
wf1									
$t_{SchenkEll}$	20,08	1,24	18,84	39,64	N	1,242	m	16,45	Nm
$t_{Schenk\ Bell}$	20,64	1,24	19,40	32,67	N	1,242	m	9,30	Nm
wf2									
$t_{SchenkEll}$	13,00	0,55	12,45	20,81	N	1,808	m	4,67	Nm
$t_{Schenk\ Bell}$	10,33	0,55	9,78	13,27	N	1,808	m	1,79	Nm
wf3									
$t_{SchenkEll}$	6,47	0,40	6,08	8,36	N	2,270	m	0,82	Nm
$t_{Schenk\ Bell}$	3,39	0,40	2,99	3,49	N	2,270	m	0,18	Nm
wf4									
$t_{SchenkEll}$	2,44	0,16	2,28	2,28	N	2,628	m	0	Nm
$t_{Schenk\ Bell}$	0,67	0,16	0,50	0,50	N	2,628	m	0	Nm

This also leads to a bending moment (Bm) at every wing section. The bending moment is defined as Force * Lever arm (McCaw, 2014). The Bm at the wingtip is zero. The Bm of the next wing section is the Bm of the previous one plus the Q values of the previous section multiplied with the distance to that wing segment. This again was repeated for all segments until the wing root. The torsion moments are not calculated and should be focus of another study. All results calculated with $n_{pos} = 1$, are shown in Table 11. A positive bending moment means a dorsal displacement and bend of the wing in this case. Another simpler method was also used to calculate the bending

moment. The assumption was made that each wing has to generate the force of half the body weight. This gives the equation: Lift*L_lift = Bm. L is the lift generated by one wing or half the

body weight and L_lift is the lever of the wing, which is assumed to be equivalent to the aerodynamic center of a right-angled triangular wing. L_lift = half wingspan * 1/3. This gives a bending moment of 76,68 Nm.

6.9 Muscle Force Calculations

The pectoral muscle is the primary depressor of the wing and it has to generate a certain amount of force to hold the wing in a gliding position and prevent it from dislocating dorsally. Assuming that the bending moment in the shoulder has to be equal to the lever of the pectoral (Plever) muscle multiplied with the force (Fpect) it generates. The pectoral force was the unknown variable. The lever of the muscle is the distance between the muscle and the point of rotation, in this case the shoulder joint, best seen in Figure 17. The lever for the muscle was calculated using the simple trigonometric function: cosθ = Adjacent/Hypotenuse. The angle of the pectoral muscle is 28° and the point where the pectoral muscle originates is at roughly one third of the humeral length. Plever is 0,037 m With all variables known the equation can be changed and written as follows: Bm(shoulder)/Plever = Fpect.

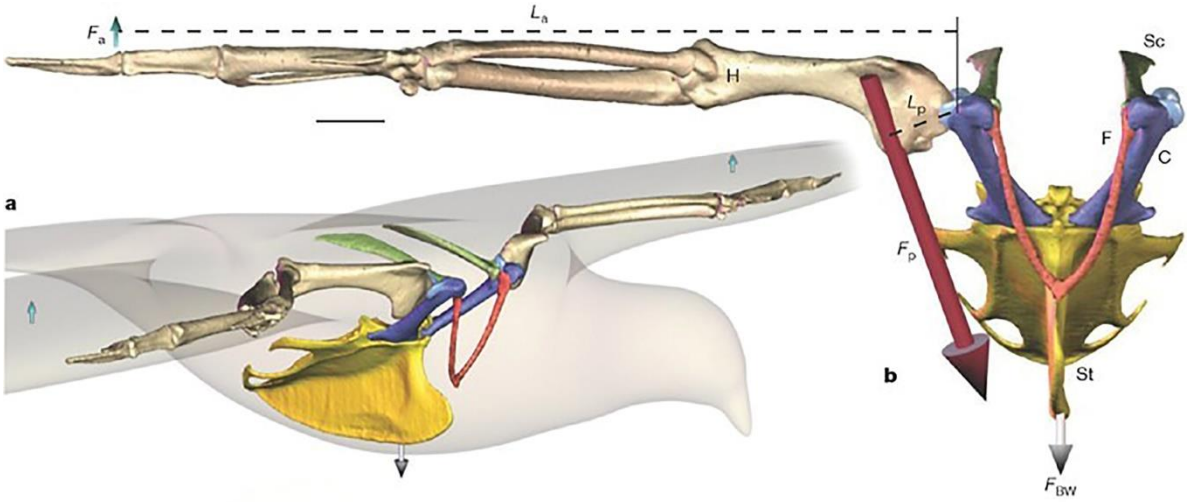

Figure 17: Forelimb skeleton and pectoral girdle of a pigeon during gliding. The same principles and forces can be applied to the pectoral girdle of *Anhanguera*. Fa – aerodynamic forces , La - lever arm for Fa, Lp - lever arm pectoralis, Fp - pectoralis force, H - humerus, F - furcula, C - coracoid, Sc - scapulacoracoid, St - sternum ,F_{BW} - birds body weight , (changed from Baier, Gatesy & Jenkins, 2007)

The equation was used for both lift distribution scenarios. At an angle of 28° of pectoral muscle inclination the force the muscle has to generate is 1 938,26 N for the

elliptical distribution and 1 596,56 N for the bell shaped distribution which is 18% lower. For the simpler method the same method was used and the result is 2 036,70 N and therefore closer to an elliptical distribution than to a bell shaped. The same was done for gliding at 2,3 and 2,52 G-forces. At 2,3 G-forces the pectoral muscle has to generate 4 458,01 N; 3 672,08 N and 4 684,42 N for the elliptical distribution, bell shaped distribution and the simple method respectively. At 2,52 times the earth acceleration the values go up to 4 884,43 Newton for the elliptical distribution, 4 023,33 N for the bell shaped distribution and 5 132,50 N for the simple method distribution. The results show that a change in lift distribution reduces the force requirements for the pectoral muscle by a good amount. This could have been applied by pterosaur by either changing the tension of the membrane, the angle of attack of different segment or a combination of both. The muscle forces presented here would not represent the peak performance of the muscle as it only shows the peak isometric forces of the muscle. Normal gliding at one g-force the muscle has to generate nine times the body weight in the bell distribution scenario which would be in line with those experienced by birds during flight. For the simple method the values increase to 12 time the body weight. In birds (Pigeon, *Columba livia*) the pectoralis has to generate a force equal to seven times the body weight during soaring and up to 13 times the body weight during flapping. It has to be stated that in this study the same approach as the simple method approach in this study was used to calculate the pectoral force. The real forces produced by the pectoral muscle can therefore be lower in reality. At 2,52 G-forces the values increase to almost 25 times the bodyweight and up to 31 times the bodyweight in the simple method, which is not reported for birds (Baier, Gatesy & Jenkins, 2007). Baier, Gatesy & Jenkins (2007) looked at the shoulder joint of alligators and stated the possibility that: “…..shoulder joint stabilization evolved within archosaurs from a primarily active, muscle-based balance system to a passive, ligament-based system in extant, volant birds.” (Baier , Gatesy & Jenkins Jr 2007: 308). This could be a reason that would explain the high percentage of pectoral muscles mass compared to the total body weight. In Birds the pectoral muscle mass makes up 6-16 % of the body mass depending on the species (Edwards, 1886). In the model used in this study the *m. pectoralis* makes up 32% of the total body mass and would therefore be able to withstand and generate more force. A bigger and more powerful chest muscle not only would have been used to stabilize the shoulder but for take-off (Habib, 2008). The pectoral muscle is not only pulling the humerus down but because of it´s angle, also into the glenoid fossa of the scapulacoracoid. Knowing the force of the pectoral muscle

and the angle of its attack, the horizontal (Fh) and vertical (Fv) parts of the vector could be calculated, again using simple trigonometric functions. Fh = Fpect*cos(α); Fv = Fpect*sin(α)-Lift. The horizontal force generated by the pull of the *m. pectoralis* is 1 409,68 N (bell distribution) or 1 798,30 N (simple method) at one G up to 3 552,39 N (bell distribution) and 4 531,73 N (simple method) at 2,52 G.

The stresses can be calculated when the surface area of the bone is known. To approximate the area and to find a way to calculate it, the best approach is to make the surface area fit in a simple geometric shape. Thus, the humeral surface area was approximated to be equal with half the area of a rectangle. The sides a and b where measured using Blender 2.79, with a being 4 cm and b 6 cm and give a surface area of 0,0012 m^2.

During soaring at one G the pull of the pectoral muscle generates a pressure of 1 174 730,76 N/m^2 (Pa) or 1,17 MPa for the bell scenario and 1 498 586,40 N/m^2 in the simple method scenario. At 2,52 G the pressure increases to 2,96 MPa and 3,78 MPa. The cartilage in the glenohumeral joint should have been able to withstand those forces as the peak normal stresses across species today lies in the range of 0.5 to 5.0 MPa (Brand, 2005). It is not clear how much cartilage extinct archosaurs possessed but some studies suggest that because of the simply shaped articular surfaces, large amount of cartilage where present in those groups. (Holliday, Ridgely, Sedlmayr, & Witmer, 2010). If this also applies to pterosaurs should be subject to another study. At last, it has to be stated that some studies of modern volant birds show that, peak forces of the pectoral muscle never exceeded 39% of the peak isometric force, even during flight at or near the maximal performance (Biewener & Dial, 1995)

7 Conclusion

The data presented in this thesis shows that the relative force the pectoral muscle generated in *Anhanguera piscator* during different gliding scenarios would be significantly higher than in modern birds. This means that the Null-Hypothesis would be rejected by these results. The cartilage should have been able to withstand the forces produced by the pull of *m. pectoralis.* The method used in this thesis can be applied to all species of pterosaurs but doesn´t present a 100% valid estimation of the body mass, as the muscle mass reconstructed here is only an estimation. To further improve the accuracy of this study, each wing segment should have its specific airfoil that should be analyzed. The lift distribution used in this thesis only represents a gliding scenario. To calculate the forces exerted by the pectoral muscle during the down stroke, a different distribution should be used. The results obtained by this study can be applied in a Finite Element Analysis (FEA) to the humerus to study how it reacts to the force and what the breaking limits of the deltopectoral crest are. The same method used for the glenohumeral joint can also be applied to any other joint in the arm but most importantly to the elbow joint.

8 Acknowledgments

First of all, I would gratefully thank my supervisor Dr. Jürgen Kriwet for his committed support as much as Gareth Dyke and Colin Palmer for the idea for this thesis. I also thank Dipl.-Ing. Manfred Milkovits for the support and for the help with the lift calculations. I thank Valentin Perlinger and Roland Mayer for helping me to prepare the casts. I also thank Christoph Kettler for turning the physical model into a 3D model. Many thanks to Marcelo and Sabine Merwald-Schmitzer, Sandy Schmitzer, Stefan and Bernadette Dressler-Stross, Christoph Weidinger, Marion Schmitzer, Yvonne Dvorak, Claudia Schmitzer, Fritz Salzer, Anton Wegan, Nina Jokic, Josephine Wegan, Martin Wegan, Chago and Mia Merwald-Schmitzer, Michael Haider, Nina Brandstätter and Harald Auer for their support.

9 References:

Abbott M., Willits P., Kailey L., 1993. Private pilot manual. Englewood.

Baier D. B., Gatesy S. M. and Jenkins F. A., 2007. A critical ligamentous mechanism in the evolution of avian flight. Nature, 445(7125), pp.307–310.

Bennett C. S., 2003. Morphological evolution of the pectoral girdle of pterosaurs: Myology and function. – In: E. Buffetaut & J.- M. Mazin (Eds.), Evolution and Palaeobiology of Pterosaurs. Geological Society Special Publications 217; London (Geological Society of London), 191–215.

Bennett, C. S., 2008. Morphological evolution of the wing of pterosaurs: Myology and function. Zitteliana Reihe B: Abhandlungen der Bayerischen Staatssammlung fur Palaontologie und Geologie, (28), pp.127–141.

Benton, M.J., 2014. Vertebrate palaeontology 4. ed., Malden, Mass. [u.a.]: Blackwell.

Biewener, A.A. and Dial, K.P., 1995, In vivo strain in the humerus of pigeons (*Columba livia*) during flight. J. Morphol., 225: 61-75.

Brand, R.A., 2005. Joint contact stress: a reasonable surrogate for biological processes. The Iowa orthopaedic journal, 25, pp.82–94.

Campos D. A., Kellner A. W. A., 1985. Panorama of the flying reptiles study in Brazil and South America. Anais da Academia Brasileira de Ciências 57:453–466.

Campos D. A. and Kellner A. W. A., 1985. Panorama of the flying reptiles study in Brazil and South America. Anais da Academia Brasileira de Ciências 57(4):453-466.

Edwards C.L., 1886. The Relation of the Pectoral Muscles of Birds to the Power of Flight. The American naturalist, 20(1), pp.25–29.

Elgin R. and Frey A., 2011., A new ornithocheirid, *Barbosania gracilirostris* gen. et sp. nov. (Pterosauria, Pterodactyloidea) from the Santana Formation (Cretaceous) of NE Brazil. Swiss Journal of Palaeontology, 130(2), pp.259–275.

English L.T and MiddletonK.M, 2015. Challenges and advances in the study of pterosaur flight. Canadian Journal of Zoology, 93(12), pp.945–959.

Eslinger, B., Murillo O. J., Jensen R., Gelzer C., and Bowers A. H., 2016. On Wings of the Minimum Induced Drag: Spanload Implications for Aircraft and Birds. NASA/TP-2016-219072.

Georgantopoulou, C. G. and Georgantopoulos, G. A., 2018. International Standard Atmosphere, SI Units. In Fluid Mechanics in Channel, Pipe and Aerodynamic Design Geometries 2. Hoboken, NJ, USA: John Wiley & Sons, Inc., pp. 239–249.

Gignac, P.M. and Erickson, G.M., 2016. Ontogenetic bite-force modeling of *Alligator mississippiensis*: implications for dietary transitions in a large-bodied vertebrate and the evolution of crocodylian feeding. Journal of Zoology, 299(4), pp.229–238.

Habib M., 2008. Comparative evidence for quadrupedal launch in pterosaurs. Zitteliana Reihe B: Abhandlungen der Bayerischen Staatssammlung fur Palaontologie und Geologie. (28), pp.159–166.

Holliday, C. M, Ridgely, R. C, Sedlmayr, J.C, and Witmer, L. M., 2010. Cartilaginous Epiphyses in Extant Archosaurs and Their Implications for Reconstructing Limb Function in Dinosaurs. PloS one, 5(9), p.e13120.

Kassera, W., 1991. Flug ohne Motor : ein Lehrbuch für Segelflieger. 11. Auflage, Stuttgart: Motorbuch-Verlag.

Kellner W. A. and Tomida Y., 2000. Description of a new species of Anhangueridae (Pterodactyloidea) with comments on the pterosaur fauna from the Santana

Formation (Aptian-Albian), northeastern Brazil. National Science Museum Monograph 17:1-135.

Kraus K., 2007. Photogrammetry: Geometry from Images and Laser Scans Originally. Berlin, Boston: DE GRUYTER.

Kühr W., 1996. Der Privatflugzeugführer, Band 1: Technik. Luftfahrtverlag, Bergisch Gladbach, Germany.

Martin E.G. and Palmer, C., 2014. A novel method of estimating pterosaur skeletal mass using computed tomography scans. Journal of Vertebrate Paleontology, 34(6), pp.1466–1469.

Martin, E.G., Palmer, C. and Claessens, L., 2014. Air Space Proportion in Pterosaur Limb Bones Using Computed Tomography and Its Implications for Previous Estimates of Pneumaticity. PLoS ONE, 9(5), p.e97159.

McCaw S., 2014. Biomechanics for dummies, Hoboken, NJ: Wiley.

Naish, D. and Witton, M.P., 2017. Neck biomechanics indicate that giant Transylvanian azhdarchid pterosaurs were short-necked arch predators. PeerJ, 5(1), p.e2908.

O. Schrenk, 1940. Ein einfaches Näherungsverfahren zur Ermittlung von Auftriebsverteilungen längs der Tragflügelspannweite. Luftwissen; Bd. 7, Nr. 4, pp.118–120.

Palmer C., 2015. Flexible fliers: the flight of pterosaurs. unpublished PhD thesis, University of Bristol.

Palmer, C. and Dyke, G., 2012. Constraints on the wing morphology of pterosaurs. Proceedings of the Royal Society B, 279(1731), pp.1218–1224.

Palmer, C. and Dyke, G.J., 2010. Biomechanics of the unique pterosaur pteroid. Proceedings of the Royal Society B, 277(1684), pp.1121–1127.

Pinheiro F. L. and Rodrigues T., 2017. Anhanguera taxonomy revisited: is our understanding of Santana Group pterosaur diversity biased by poor biological and stratigraphic control? PeerJ, 5(5), p.e3285.

Prandtl L., 1921. Applications of modern hydrodynamics to aeronautics, NACA Report No 116 Washington, DC.

Prandtl L., 1933. Über tragflügel kleinsten induzierten widerstandes. Zeitschrift für Flugtecknik und Motorluftschiffahrt, München, Germany.

Simons E. L. R., 2009. The Evolution of Forelimb Morphology and Flight Mode in Extant Birds, PhD Thesis, Ohio University, USA.

Sullivan, S.P., McGechie, F., Middleton, K., and Holliday, C, 2019. 3D Muscle Architecture of the Pectoral Muscles of European Starling (Sturnus vulgaris). Integrative Organismal Biology, 1(1), pp.Integrative Organismal Biology, 2019, Vol. 1(1).

Unwin, D.M., 2006. Pterosaurs : from deep time 1. print., New York, NY: PI Press.

Wilkinson M.T., 2008. Three-dimensional geometry of a pterosaur wing skeleton, and its implications for aerial and terrestrial locomotion. Zoological Journal Of The Linnean Society, 154(1), pp.27–69.

Witton M. and Habib M., 2010, On the Size and Flight Diversity of Giant Pterosaurs, the Use of Birds as Pterosaur Analogues and Comments on Pterosaur Flightlessness. PloS one, 5(11), p.e13982.

Witton M., 2013. Pterosaurs : : Natural History, Evolution, Anatomy, Princeton, N.J. : Princeton University Press.

Witton M., 2008 A new approach to determining pterosaur body mass and ist implications for pterosaur flight. Zitteliana B28: 143 – 159.

Websides:

Agisoft, n.d. Features. www.agisoft.com (accessed 03.07.2020).

American Museum of National History, 2007. Division of paleontology www.research.amnh.org/paleontology/search.php?action=image_detail&specimen_id=36867# (accessed 04.12.2019).

Blender, n.d. The Software. http://www.blender.org/about (accessed 25.06.2020).

Fossilworks, n.d. Chapada do Araripe, Romualdo Member (general) (Cretaceous of Brazil). www.fossilworks.org/?a=collectionSearch&collection_no=92290&is_real_user = 1 (accessed 24.02.2020).

Lions Club Frankfurt am Main, 2013. Wissenswertes. www. frankfurt-am-main.lc-cms.de/index.php/der_club-wissenswertes (accessed 01.11.2020).

MATLAB, 2020. What is MATLAB. www.mathworks.com/discovery/what-is-matlab.html; (accessed 23.06.2020).

University of Michigan, 2008. Birds, Bats And Insects Hold Secrets For Aerospace Engineers. ScienceDaily. www.sciencedaily.com/releases/2008/02/ 080204172203.htm (accessed 08.09.2020).

XFLR5, 2019. General description. www.xflr5.tech/xflr5.htm (accessed 29.06.2020).